Full title: Differential regulation of human bone marrow mesenchymal stromal cell chondrogenesis by Hypoxia Inducible Factor-1α hydroxylase inhibitors

Running Title: HIF-1α-stabilising agents for chondrogenesis

Author List: Dheraj K. Taheem[1], Daniel A. Foyt[1], Sandra Loaiza[2], Silvia A. Ferreira[1], Dusko Ilic[3], Holger W. Auner[2], Agamemnon E. Grigoriadis[1], Gavin Jell[4], Eileen Gentleman[1]*

1. Centre for Craniofacial and Regenerative Biology, King's College London, London SE1 9RT, UK
2. Cancer Cell Protein Metabolism Group, Department of Medicine, Imperial College London, London W12 0NN, UK
3. Division of Women's Health, Women's Health Academic Centre KHP, King's College London, London, UK
4. Division of Surgery & Interventional Science, University College London, London NW3 2QG, UK

*To whom correspondence should be addressed: **Address**: Centre for Craniofacial & Regenerative Biology, Floor 27, Tower Wing, Guy's Hospital, King's College London, London, SE1 9RT UK, **Tel**: +44 (0) 20 7188 7388, **Email**: eileen.gentleman@kcl.ac.uk

Author contributions

Dheraj K. Taheem: Conception and design, collection and assembly of data, data analysis and interpretation, wrote the manuscript.

Daniel Foyt: Collection and assembly of data, revised the manuscript.

Sandra Loaiza: Provision of hBM-MSC, revised the manuscript.

Silvia Ferreira: Collection and assembly of data, revised the manuscript.

Dusko Ilic: Conception and design, data analysis and interpretation, revised the manuscript.

Holger W. Auner: Provision of hBM-MSC, revised the manuscript.

Agamemnon E. Grigoriadis: Conception and design, data analysis and interpretation, revised the manuscript.

Gavin Jell: Conception and design, data analysis and interpretation, revised the manuscript.

Eileen Gentleman: Conception and design, data analysis and interpretation, wrote the manuscript, final approval of manuscript

Significance Statement

The repair of damaged cartilage with engineered tissues may be hampered by challenges stemming from the need to provide appropriate environmental cues to progenitor cells. By chemically targeting the Hypoxia Inducible Factor complex to mimic the effects of hypoxia, we show that the 2-oxoglutarate (2-OG) analogue DMOG induces HIF signalling and a more articular chondrocyte-like expression profile in human BM-MSC compared to $CoCl_2$ or DFX, which reduce Fe^{2+} bioavailability. These observations suggest that human BM-MSC may rely more on mechanisms that utilise 2-OG than Fe^{2+} during chondrogenesis and suggest that DMOG could be effective therapeutically for cartilage regeneration.

Abstract

The transcriptional profile induced by hypoxia plays important roles in the chondrogenic differentiation of marrow stromal/stem cells (MSC) and is mediated by the Hypoxia Inducible Factor complex. However, various compounds can also stabilise HIF's oxygen-responsive element, HIF-1α, at normoxia and mimic many hypoxia-induced cellular responses. Such compounds may prove efficacious in cartilage tissue engineering, where microenvironmental cues may mediate functional tissue formation. Here, we investigated three HIF stabilising compounds, which each have distinct mechanisms of action, to understand how they differentially influenced the chondrogenesis of human bone marrow-derived MSC (hBM-MSC) *in vitro*. hBM-MSCs were chondrogenically-induced in TGF-β_3-containing media in the presence of HIF-stabilising compounds. HIF-1α stabilisation was assessed by HIF-1α immunofluorescence staining, expression of HIF target and articular chondrocyte specific genes by qPCR, and cartilage-like extracellular matrix (ECM) production by immunofluorescence and histochemical staining. We demonstrate that all three compounds induced similar levels of HIF-1α nuclear localisation. However, whilst the 2-oxoglutarate analogue Dimethyloxalylglycine (DMOG) promoted upregulation of a selection of HIF target genes, Desferrioxamine (DFX) and Cobalt Chloride ($CoCl_2$), compounds that chelate or compete with Fe^{2+}, respectively, did not. Moreover, DMOG induced a more chondrogenic transcriptional profile, which was abolished by Acriflavine, an inhibitor of HIF-1α-HIF-β binding, whilst the chondrogenic effects of DFX and $CoCl_2$ were more limited. Together, these data suggest that HIF-1α function during hBM-MSC chondrogenesis may be regulated by mechanisms with a greater dependence on 2-oxoglutarate than Fe^{2+} availability. These results may have important implications for understanding cartilage disease and developing targeted therapies for cartilage repair.

Abbreviations

2-Oxoglutarate (2-OG)

Acriflavine (ACF)

Bone Marrow-derived Mesenchymal Stem Cells (BM-MSCs)

Chondrogenic Differentiation Media (CDM)

Cobalt Chloride ($CoCl_2$)

Collagen Prolyl Hydroxylase (CP4HA1)

Desferrioxamine (DFX)

Dimethyloxalylglycine (DMOG)

Divalent iron (Fe^{2+})

Double stranded Deoxyribonucleic Acid (dsDNA)

Extracellular Matrix (ECM)

Factor Inhibiting Hypoxia Inducible Factor (FIH)

Foetal Bovine Serum (FBS)

Glycosaminoglycans (GAGs)

Growth Media (GM)

Hypoxia Inducible Factor (HIF)

Mesenchymal Stem Cells (MSCs)

Messenger Ribonucleic Acid (mRNA)

Oxygen (O_2)

Prolyl Hydroxylase 2 (PHD2)

Quantitative Polymerase Chain Reaction (qPCR)

Room Temperature (RT)

Transforming Growth Factor-β (TGF-β)

Introduction

Acute lesions to the articular cartilage that do not heal may be painful and can progress to osteoarthritis. Conventional treatments such as microfracture or articular chondrocyte implantation are not always effective in mediating repair [1, 2]. Tissue engineering strategies that combine cells with bioactive factors and biomaterial scaffolds may allow for *de novo* articular cartilage formation and provide an alternative therapy for patients [3-5]. However, the provision of cues that can appropriately direct progenitor cell differentiation and tissue formation remain a challenge.

One of the regulatory factors controlling articular cartilage development is the cellular response to physiological hypoxia [6, 7]. The cellular response to hypoxia is mediated by the hypoxia inducible factor [8] pathway which induces expression of hypoxia-responsive genes [9]. At normoxia, the HIF complex is unable to recruit the oxygen-responsive HIF-1α subunit, which inhibits expression of genes containing a HIF response element within their promoter regions [10]. Under hypoxic conditions, HIF-1α translocates to the nucleus where it complexes with other components of the HIF complex to initiate transcription of HIF target genes [10]. HIF-1α is central in the formation of articular cartilage during development [6, 7]. It also plays essential roles in the differentiation of mesenchymal stem/stromal cells (MSC) [11, 12] and chondroprogenitors [13] into cells capable of producing cartilage-like extracellular matrix (ECM) [14-16]. Moreover, HIF-1α is vital in maintaining the articular phenotype of differentiated chondrocytes and inhibiting hypertrophic differentiation [17]. Two hydroxylases, prolyl hydroxylase 2 (PHD2) and factor inhibiting HIF (FIH), regulate the participation of HIF-1α in the HIF complex [18, 19]. Each catalyses the hydroxylation of specific residues on HIF-1α by utilising molecular oxygen (O_2) as a substrate together with ascorbic acid, iron (Fe^{2+}) and 2-oxoglutarate (2-OG). PHD2-mediated proline hydroxylation

results in ubiquitination of HIF-1α and its subsequent proteasomal degradation, whereas asparagine hydroxylation by FIH prevents HIF-1α from binding to the co-factor, p300 in the HIF complex [18]. Under hypoxic conditions, the lack of oxygen reduces PHD2 and FIH activity, enabling HIF-1α to accumulate in the nucleus and form an active transcriptional complex with co-factors at the promoter regions of HIF target genes.

The importance of hypoxia and HIF in cartilage development and maintenance point towards its potential utility in cartilage tissue engineering strategies. Indeed, chemical agents that upregulate HIF have been shown to drive the chondrogenic differentiation of MSC and promote articular chondrocytes to produce a cartilage-like ECM [12, 20, 21]. However, studies which compare the efficacy of different HIF-stimulating compounds in driving the chondrogenesis of hBM-MSC compared to standard protocols which utilise transforming growth factor-β (TGF-β), are lacking.

Therefore, we compared the effects of three hydroxylase inhibitors on the chondrogenic differentiation of hBM-MSC. Dimethyloxalylglycine (DMOG) strongly binds to the 2-OG binding pocket of both FIH and PHD2, acting as a competitive inhibitor [22]; Desferrioxamine (DFX) sequesters intracellular Fe^{2+}, which is required by FIH and PHD2 [23], and thereby reduces their activity; and Cobalt Chloride ($CoCl_2$) competes with Fe^{2+} by directly binding to the PHD2 active site [24]. We chose these agents because they cover the main classes of HIF-stimulating compounds, and as such, upregulate HIF-1α via distinct mechanisms (Figure 1A+1B). These compounds are also the most widely studied for chemically regulating HIF and may shed light on key regulatory elements of hypoxic signalling during chondrogenesis. Moreover, investigating the PHD2/FIH inhibitors during hBM-MSC chondrogenesis may aid our understanding of the pathophysiology of degenerative diseases such as osteoarthritis [8], for which HIF-1α is known to play a protective role [25].

Here, we show that whilst $CoCl_2$, DFX and DMOG all induce similar levels of HIF-1α stabilisation, only DMOG strongly enhances HIF-mediated transcription of key chondrogenic genes. Nevertheless, DMOG negatively impacted the production of Collagen Type II and glycosaminoglycans (GAGs), which could be alleviated by only exposing cells to the compound during the latter stages of chondrogenesis. Together, these observations highlight the potential importance of mechanisms which utilise 2-OG compared to Fe^{2+} for the transcriptional control of HIF target genes during hBM-MSC chondrogenesis. They also suggest that 2-OG inhibitors may better promote a chondrogenic transcriptome compared to either DFX or $CoCl_2$. These observations may inform on improved, targeted strategies for stimulating cartilage ECM formation in tissue engineering-based therapies.

Materials & Methods

Isolation and expansion of hBM-MSC

hBM-MSCs were isolated from bone marrow aspirates collected from the iliac crest of healthy paediatric donors, with informed consent from their parents or guardians. Cells were seeded in CellSTACK® (Corning) culture chambers at 10-25x10^6/636 cm^2 and cultured in αMEM supplemented with human platelet lysate (Stemulate, Cook Medical, USA). At 90-100% confluency, cells were passaged and seeded at 5000 cells/cm^2. For immunophenotyping of hBM-MSCs, the following antibodies were used in conjunction with a FACSCalibur™ analyser (BD Biosciences): CD90-FITC, CD105-APC, CD73-PE, CD34-PE, and CD45-FITC (all from BD Biosciences). All human tissue was approved for use by the UK National Research Ethics Service (12/WA/0196) and was collected by the National Institute for Health Research, which is supported by the Imperial College Healthcare Tissue Bank (HTA license 12275). Cultures were found to express CD90, CD105, CD73 and not express hematopoietic markers CD34 and CD45 [26] (data not shown). hBM-MSCs were

expanded in growth media (GM; αMEM + 10% Foetal Bovine Serum (FBS)) under standard conditions (5% CO_2).

Chondrogenic Induction of hBM-MSC

hBM-MSCs were expanded to passage 5 in GM under standard culture conditions before cryopreservation in a solution composed of 10% Dimethyl Sulfoxide, 40% FBS and 50% GM. Cells were stored in liquid nitrogen prior to use. For chondrogenic induction experiments, cryovials of hBM-MSCs were thawed in GM and grown to confluence before plating at $3x10^4/cm^2$ into multi-well tissue culture plates. Cultures were incubated for 24 h in GM prior to induction using standard chondrogenic differentiation media (CDM). See Figure 1C for experimental plan. Cells were differentiated as monolayers to prevent the formation of a local hypoxic microenvironment independent of experimental conditions (physiological or chemically-induced hypoxia). Indeed, whilst pellet/micromass cultures may be more conducive for chondrogenesis, the bioavailability of oxygen may vary between cells at the periphery and centre of such cultures. CDM consisted of High Glucose Dulbecco's Modified Eagle Medium (Sigma Aldrich) + 2mM L-Glutamine (Thermo Fisher Scientific) + 100nM Dexamethasome (Sigma Aldrich) + 1% Insulin, Transferrin, Selenium Solution (Thermo Fisher Scientific) + 1% Antibiotic Antimycotic solution (Sigma Aldrich) + 50μg/ml Ascorbic acid-2-phosphate (Sigma Aldrich) + 40μg/ml L-proline (Sigma Aldrich) + 10ng/ml TGF-β_3 (Peprotech). CDM was supplemented with HIF-stabilising compounds (Sigma Aldrich): 100μM $CoCl_2$, 50μM DFX and 200μM DMOG, or incubated in un-supplemented CDM at hypoxia (5%O_2) or normoxia. To achieve HIF-1α inhibition, media was further supplemented with 500nM Acriflavine (ACF; Santa Cruz).

Neutral Red Viability Assay

Neutral red dye (Sigma-Aldrich) dissolved in cell culture medium was incubated with differentiating hBM-MSC for 2 h before fixation in 0.1% Calcium Chloride+0.5% paraformaldehyde. Dye retained by hBM-MSC was solubilised in 1% acetic acid + 50% ethanol. Quantification of solubilised Neutral Red was then performed on an absorbance spectrophotometer at 540nm.

PicoGreen Assay

Samples were snap-frozen at -80 °C and digested in 400μg/ml Papain Buffer at 65 °C for 18 hours. Double stranded Deoxyribonucleic Acid (dsDNA) content in papain-digested cultures was quantified using a PicoGreen kit (Thermo Fisher Scientific). A linear relationship was observed between hBM-MSC number and dsDNA content.

SDS-PAGE & Western Blotting

Following 24-hours of culture, cells were lysed in Sodium Dodecyl Sulfate (SDS) buffer and protein was quantified using a Bicinchoninic Acid assay (Thermo Fisher Scientific). Lysates were run on polyacrylmide gels (Biorad) and transferred using the Trans-Blot Turbo Transfer System (Biorad). HIF-1α and housekeeping protein β-Actin were bound by primary antibodies (h-206; Santa Cruz and ab8227; Abcam). Signal detection produced between a horseradish peroxidase-conjugated secondary antibody (sc-2004; Santa Cruz) and the Chemiluminescent ECL substrate (Biorad) were detected on a Chemidoc Touch imaging platform (Biorad). HIF-1α and protein levels were generated by densitometric analysis with ImageJ and normalised to that of β-Actin.

Quantitative Polymerase Chain Reaction

RNA was extracted using the RNeasy Mini Kit (Qiagen). 100ng of RNA per sample was reverse transcribed using M-MLV Reverse Transcriptase (Promega) and cDNA was amplified using quantitative polymerase chain reactions (qPCR) in a CFX384 (Biorad). Brilliant III Ultra-Fast SYBR® Green QPCR Master Mix (Agilent) was used in conjunction with primers specific to genes of interest. Primer sequences are shown in Supplemental Table 1. All primers produced a linear relationship between template concentration and Ct value. Reaction efficiencies were confirmed to always be between 90 and 110%. Raw Ct values were converted to transcript copy number by the relative standard curve method of analysis, and expression levels were normalised to that of *RPL13A*. Following normalisation to the housekeeping gene, expression levels were then normalised to that of the untreated control to determine fold change in expression induced by each treatment.

Immunofluorescence Staining

Cultures were fixed in 4% (w/v) paraformaldehyde for 15 minutes. HIF-1α and Collagen Type II were then detected using h-206 (Santa Cruz) and ab34712 (Abcam) (respectively), overnight, following blocking with (10%) goat serum (Sigma Aldrich) for 60 min and permeabilisation in 0.1% (v/v) Triton X-100 solution (Sigma Aldrich) for 60 min, both at room temperature (RT). Collagen Type X was detected using ab49945 (Abcam) at a 1:250 dilution overnight. Rabbit-derived primary antibodies were visualised with ab150077 (Abcam) after staining for 60 min at RT at dilutions of 1:000 and 1:200 for Collagen Type II and HIF-1α, respectively. Mouse-derived primary antibodies were detected with biotin (ab6788, Abcam) and Streptavidin (S11223, Thermo Fisher Scientific) both at 1:350 for 60 min. Cultures were counterstained with 0.1μg/ml DAPI for 60 min to visualise nuclei and fluorescence was imaged on an Axiovert200M microscope (Zeiss). The images in

Supplemental Figure 1 confirm that signal was due to each primary antibody and not background fluorescence or non-specific binding of the secondary antibody.

Alcian Blue Staining

4% paraformaldehyde-fixed cultures were stained with 1% Alcian Blue solution, pH 1.0 (Sigma Aldrich) prepared in 0.1N HCl. Haematoxylin (Vector Laboratories) was used to visualise cell nuclei and staining was imaged on an Axiovert200M microscope (Zeiss).

Glycosaminoglycan Quantification

At day 21 of chondrogenesis, cultures were washed in PBS and frozen at -80 °C before their digestion in 400μg/ml Papain buffer (Sigma Aldrich) supplemented with 0.2M Sodium Phosphate + 5mM Ethylenediaminetetraacetic acid + 5mM L-Cysteine (all Sigma Aldrich) at 65 °C for 18 h. Glycosaminoglycans were quantified from Papain-digested lysates using the GAG assay kit by *Blyscan*™ in which GAGs were dyed with 1,9-dimethyl-methylene blue and subsequently dissociated with Propan-1-ol solution before quantification on an absorbance spectrophotometre at 640nm. Values were normalised to levels of dsDNA, which were quantified using the PicoGreen assay.

Immunofluorescence Quantification

Immunofluorescence images were captured using identical gain, exposure and offset for all conditions in each experiment. These were determined with positive controls that expressed the antigen of interest, and negative controls in which the primary antibody was omitted (Supplemental Fig. 1). The same threshold fluorescence intensity for images of all conditions within an experiment was set, below which the signal produced was negated as background. The signal produced above the threshold was regarded as *bona fide* protein detection and was

used to create a binary representation of each image. The percentage of immunofluorescence staining present within a specified area was then determined.

Statistical Analysis

All statistical analyses were performed in Prism7 (GraphPad) with the Mann-Whitney test used to compare two conditions and Kruskal-Wallis with Dunn's Correction for multiple condition comparisons. Non-parametric tests were used as we were unable to demonstrate normality in all datasets. *marks all differences that were statistically significant ($p<0.05$).

Results

Hypoxia promotes HIF stabilisation and a more articular cartilage-like cell phenotype

It is well established that hBM-MSCs can be chondrogenically differentiated with transforming growth factor β_3 (TGF-β_3) ligands. Therefore, we first aimed to determine if chondrogenesis could be further enhanced by culture under hypoxic conditions, as previously reported [11]. Hypoxia increased messenger Ribonucleic Acid (mRNA) expression of a selection of known HIF target genes including *VEGFA*, *EGLN*, and *PGK1* (all $p=0.0286$) [27-29] compared to that in hBM-MSC cultured under normoxic conditions (Figure 2A). These observations were in line with previous studies which have similarly shown a rapid (24 h) upregulation of HIF and HIF-mediated transcription in response to hypoxia under chondrogenic conditions [11]. However, 5%O_2 did not significantly affect expression of *SOX9* (Figures 2A+2B; $p=0.1$), the master transcriptional regulator of chondrogenesis [30], after either 1 or 14 days in culture.

At day 14 we observed upregulation of expression of the gene for the articular cartilage ECM component Collagen Type II (*COL2A1*, $p=0.0002$), and downregulation of the hypertrophic

marker Collagen Type X [31] (*COL10A1, p*=0.0006) under hypoxic conditions compared to that at normoxia (Figure 2B). *COL2A1* and *COL10A1* are targets of transcription factors *SOX9* and *RUNX2*, respectively, and are known to be regulated as the chondrogenic differentiation of MSC proceeds [11]. Culture for 21 days under hypoxic conditions did not affect cell viability or proliferation (Figure 2C). However, as expected, we did observe increased HIF-1α nuclear localisation ($p<0.0001$) in hypoxic compared to normoxic cultures (Figures 2D-2H). Hypoxia also increased Alcian Blue staining of GAGs (Figures 2I+2J), but did not affect the immuno-detection of Collagen Type II protein (Figures 2K+2L). Nevertheless, we did detect a decrease in staining for Collagen Type X (Figures 2M+2N), consistent with hypoxia's inhibitory role to chondrocyte hypertrophy [17]. Together, these observations confirmed that culture under hypoxic conditions in the presence of TGF-β_3 promoted an articular chondrocyte-like phenotype that was conducive for articular cartilage ECM rather than hypertrophic cartilage formation. This effect appeared to not require a corresponding upregulation of *SOX9*, but instead correlated with increased immunostaining for HIF-1α, upregulation of select HIF target genes *VEGFA*, *EGLN*, and *PGK1*, and increased HIF-1α nuclear localisation.

$CoCl_2$, DFX and DMOG induce HIF-1α localisation, but only DMOG strongly upregulates HIF targets *VEGFA*, *PGK1* and *ELGN*

Having determined that hypoxia promoted HIF-1α stabilisation and expression of *VEGFA*, *EGLN*, and *PGK1*, we next aimed to determine if inhibitors of the hydroxylases PHD2 and FIH would have a similar effect on hBM-MSC cultured under normoxic conditions. We first determined appropriate doses for the hydroxylase inhibitors DMOG, DFX and $CoCl_2$ by confirming that concentrations of each used extensively in the literature [22, 24, 32-34] were non-toxic to hBM-MSC over 21 days of chondrogenic differentiation (Supplementary Figures

2 and 3). Next, we confirmed that each could stabilise HIF by carrying out Western blots for HIF-1α in whole-cell lysates after 24 h, as HIF is known to be rapidly induced in response to PHD2/FIH inhibition [22]. Levels of HIF-1α protein were significantly increased in cells cultured under hypoxic conditions (p=0.0286); however, despite trends for increased levels of HIF-1α after treatment with HIF stabilising compounds, we failed to detect statistically significant differences (p=0.314) compared to controls (Figures 3A+3B). Nonetheless, nuclear localisation of HIF-1α was enhanced compared to controls (p=<0.0001) in response to treatment with all three compounds (Figures 3C-3K).

We then examined the effects of the hydroxylase inhibitors on HIF target gene expression. DMOG significantly and consistently upregulated expression of *VEGFA* (p= day 1: 0.0073, day 7: 0.0470, day 21: 0.0005), *PGK1 (*p= day 1: 0.0073, day 7: 0.0013, day 14: 0.0013, day 21: 0.0031) and *EGLN* (p= day 1: 0.0108, day 7: 0.0332, day 14: 0.0470, day 21: 0.0005) (Figures 3L-3N). However, the effects of $CoCl_2$ and DFX were more subtle, and we only observed upregulation of *PGK1* expression at day 14 (p=0.0391) and *EGLN* at day 21 (p=0.0396) in response to DFX. These observations show that whilst $CoCl_2$, DFX, and DMOG all affect HIF-1α stabilisation, only DMOG strongly upregulated expression of a selection of HIF target genes. This suggests that DMOG more potently enhanced HIF activity compared to DFX or $CoCl_2$.

DMOG stimulates hBM-MSC to adopt an articular chondrocyte-like transcriptional profile

As all HIF mimetics stabilised HIF-1α and DMOG also upregulated expression of HIF target genes, we next investigated the effect of these compounds on chondrogenic gene expression. DMOG treatment upregulated *SOX9* mRNA after 7 (p=0.0159) and 21 (p=0.0332) days in culture (Figure 4A), whilst *RUNX2*, a key regulator of osteogenesis [35], was unaffected

under all conditions (Figure 4B). This resulted in a DMOG-mediated increase in the *SOX9* to *RUNX2* expression ratio throughout differentiation (Figure 4C; p= day 7: 0.0192, day 14: 0.0398, day 21: 0.0159). All inhibitors upregulated expression of *COL2A1* (Figure 4D; p= $CoCl_2$: 0.0280, DFX: 0.0180, DMOG: 0.0008) with DMOG significantly downregulating *COL10A1* (Figure 4E; p=0.0037) leading to an increased *COL2A1*/*COL10A1* mRNA ratio due to DFX and DMOG (Figure 4F; p= DFX: 0.0259, DMOG: <0.0001). *ACAN*, which encodes the gene for Aggrecan, the most abundant proteoglycan in cartilage [36], was not upregulated by any treatment (Figure 4G); and *MMP13*, which contributes to an osteoarthritic chondrocyte phenotype [37], was similarly unaffected (Figure 4H). The articular cartilage phenotype is marked by appropriate post-translational modifications of secreted collagen by enzymes encoded by *P4HA1* and *LOX* [14, 15]. DMOG strongly upregulated both *P4HA1* (Figure 4I; p=0.0039) and *LOX* (Figure 4J; p=0.0027) expression, whilst DFX only upregulated *LOX* (p=0.0056) and $CoCl_2$ had no significant effects. Taken together, these observations demonstrate that DMOG upregulated transcriptional regulators of chondrogenesis and genes involved in cartilage ECM formation, whilst the effects of $CoCl_2$ and DFX were more limited.

DMOG inhibits incorporation of Collagen Type II, Type X and GAGs into the cell-secreted ECM

As treatment with DMOG regulated the expression of genes associated with a chondrocyte phenotype, we next asked if this influenced cartilage-like matrix formation. In line with changes in gene expression, hBM-MSC treated with DMOG for 21 days showed little to no staining for Collagen Type X compared to controls (Figures 5A+5D). We observed a similar effect in both DFX- and $CoCl_2$-treated cultures (Figures 5B+5C). However, whilst $CoCl_2$- and DFX-treated cultures showed similar levels of staining for Collagen Type II as controls

(Figures 5E-5G), DMOG-treated cultures showed only sparse staining (Figure 5H). This was confirmed by quantification of Collagen Type II immunofluorescence both without (p=0.0286) and with normalisation to cell number which indicated reduced Collagen Type II production per cell (Figure 5M; p=0.0286). Alcian blue staining confirmed these observations as DMOG-treated cultures showed fewer GAG-positive areas than the other groups, although quantitative differences in staining on a per cell basis were not significant (Figures 5I-5L+5N). Overall, DMOG appeared to reduce the total amount of cartilage-like ECM that cells formed in their immediate extracellular space.

HIF-1α mediates DMOG's induction of an articular chondrocyte transcriptional profile

As DMOG mediated antithetical effects in terms of chondrogenic transcriptional profile and ECM formation, we next aimed to study its mechanism of action. To accomplish this, we supplemented $CoCl_2$/DFX/DMOG-containing CDM with Acriflavine (ACF), an inhibitor of HIF-1α and HIF-1β binding [38]. ACF abolished the DMOG-induced upregulation of established HIF targets, but did not affect total cell number during chondrogenesis (Supplemental Figure 4A and Supplemental Figure 4B). Staining for Collagen Type II in DMOG-treated cultures supplemented with ACF remained sparse (Figures 6A-6C), but quantitative image analyses showed staining on a per cell basis was no different from controls, whilst cultures treated with DMOG alone were significantly lower (Figure 6D; p=0.0076). This suggests that the inhibitory role of DMOG on Collagen Type II matrix formation may be partly mediated through HIF-1α activity.

We next asked if DMOG's stimulation of the chondrogenic transcription profile in hBM-MSC was also mediated through HIF-1α. ACF abrogated DMOG-mediated changes in expression of HIF targets, *VEGFA* (Figures 6E*; p*= -ACF: 0.0132, +ACF: 0.0772) and *EGLN* (Figures 6F; *p*= -ACF: 0.0073, +ACF: 0.1232), *COL2A1* (Figure 6H; *p*= -ACF: 0.0286,

+ACF: >0.999), *COL10A1* (Figure 6I; *p*= -ACF: 0.002, +ACF: >0.3277), the *COL2A1/COL10A1* ratio (Figure 6J; *p*= -ACF: 0.0031, +ACF: >05998), and showed a similar trend for *SOX9* expression (Figure 6G; *p*= -ACF: 0.0772, +ACF: 0.5348) Interestingly, despite a lack of upregulation of *SOX9* under hypoxic conditions, we observed a negative effect of hypoxia on *SOX9* expression in the presence of ACF (Figure 6G; *p*= 0.0286). This is consistent with the observation that ACF reduced the ratio of *COL2A1*/*COL10A1* under hypoxic conditions (Figure 6J; *p*=0.0286) and suggests that hypoxia, via HIF-1α, does indeed regulate basal levels of chondrogenic targets genes, such as *SOX9*. Overall, these data suggest that HIF-1α mediated DMOG's effect on the transcriptional profile of chondrogenically induced hBM-MSC. Moreover, ACF appeared to have a larger effect on DMOG-mediated transcription than that induced by either $CoCl_2$ or DFX (Supplemental Figure 4C-4J).

Late DMOG treatment enhances chondrogenesis

As DMOG upregulated chondrogenic transcripts but continuous treatment led to reduced staining for cartilage-like matrix, we next asked if altering either the length/timing of treatment would influence ECM formation. Therefore, we next treated hBM-MSC with DMOG, DFX and $CoCl_2$ either continuously (as before) or during late (days 14-21) time periods and analysed mRNA and protein expression of ECM markers after 21 days. Late DMOG treatment did not negatively affect the secretion of Collagen Type II compared to controls (*p*=0.282), as we observed with continuous DMOG treatment (*p*=0.0188). This contrasted with treatment with either DFX or $CoCl_2$, where both continuous and late treatment had no effect on Collagen Type II secretion (*p*=>0.9999 for both, Figure 7A-7H). At the mRNA level, like continuous treatment (*p*=0.0023), late exposure to DMOG induced significant upregulation of *SOX9* (Figure 7I; *p*=0.0168). Late DMOG also upregulated expression of *P4HA1* (Figure 7J; *p*=0.0286), and HIF targets *VEGFA* (*p*=0.0358, Figure 7K)

and *EGLN* (p=0.0208, Figure 7L) as with continuous DMOG treatment (p= *P4HA1:* 0.0313, *VEGFA:* 0.0118, *EGLN*: 0.0088). In contrast, neither continuous nor late $CoCl_2$ and DFX treatment significantly affected the expression of these genes, with the exception of continuous DFX treatment on *SOX9* (p= 0.0286; Figure 7I) and *P4HA1* (p= 0.0286; Figure 7J). Taken together, late treatment with DMOG induced a similar expression profile to continuous treatment, but without negatively impacting the formation of cartilage-like ECM.

Discussion

Hypoxic conditions are known to favour articular cartilage development. The pro-chondrogenic effects of hypoxia are thought to be mediated primarily through HIF-1α via the formation of a transcriptionally-active complex at target genes [7, 12]. Therefore, we and others hypothesised that compounds that increase HIF-1α availability would promote HIF-mediated chondrogenesis. Previous studies have examined the effect of $CoCl_2$ [12], DFX [39] and DMOG [21, 40] in this context. Whilst such studies have cemented the role of HIF-1α in chondrogenesis, to our knowledge no study has yet examined their comparative effects during cartilage formation or the chondrogenic differentiation of precursors. As the inhibitors have differential mechanisms of action, comparatively studying their effects may have important implications for HIF biology and cartilage regenerative medicine. Indeed, instead of utilising physiological hypoxia for regenerative medicine, stabilising the HIF complex under normoxic conditions would remove the complex logistics required for spatial organisation of oxygen. This may be particularly valuable in engineering constructs for the repair of full osteochondral defects due to the contrasting oxygen requirements of avascular cartilage and vascularised bone [6]. HIF mimetics could also potentially avoid the undesirable HIF-independent effects of hypoxia such as the unfolded protein response and

associated cell stress [41], and could preclude the development of a tolerance to the reduced oxygen levels [42, 43].

In our control conditions, we defined hypoxia as 5%O_2 to balance its well-described pro-chondrogenic effects against its negative impacts on cell viability [44]. As expected, after 24 h in culture under hypoxic conditions, we detected upregulation of HIF target genes, as others have described [19, 45], as well as increased expression of SOX9 target *COL2A1* and downregulation *COL10A1* (day 14). We also detected an increase in staining for GAGs and reduced Collagen Type X protein formation. Surprisingly, upregulation of *SOX9* was not maintained throughout the 21-day differentiation. This is in keeping with previous reports that continued upregulation of *SOX9* expression in mouse MSC under hypoxic conditions does not correlate with upregulation of its target genes [11]. We also observed that *SOX9* expression was downregulated in the presence of ACF, perhaps suggesting that hBM-MSC cultures do rely on HIF for physiological hypoxia's downstream effects. Indeed, cells may develop a tolerance to hypoxia following the initial induction [43], and during long-term culture, hypoxia may act to maintain basal levels of expression of chondrogenic genes.

One of our most striking observations was the ability of DMOG, via HIF-1α, to induce hBM-MSC to upregulate expression of HIF target genes and chondrogenic transcripts, and downregulate mRNA encoding hypertrophic chondrocyte markers such as Collagen Type X. In comparison, neither $CoCl_2$ nor DFX stimulated similar changes, despite their ability to promote HIF-1α nuclear localisation. The stability and nuclear localisation of HIF-1α is controlled by PHD2, whereas HIF-1α co-factor binding is controlled by FIH; DMOG has been shown to inhibit both hydroxylases [22]. This is unlike the effect of iron chelators which target PHD2, but do not inhibit FIH as potently [24]. Others have shown that FIH requires higher levels of 2-OG than PHD2 to achieve the same levels of enzymatic activity [46], which may suggest an increased sensitivity of FIH than PHD2 to inhibition by 2-OG

analogues. HIF-1α activity in hBM-MSC may also be more dependent on FIH inhibition, rather than PHD2, as high levels of HIF-1α mRNA have been observed in these cells [42]. Indeed, high levels of HIF-1α transcription might compensate for decreases in HIF-1α stability due to PHD2-mediated hydroxylation. Taken together, these observations suggest that regulation of HIF-mediated transcription that is conducive for hBM-MSC articular chondrogenesis, is dependant more on 2-OG-mediated mechanisms than those controlled by intracellular Fe^{2+} levels. Additionally, previous studies which demonstrate the dependence of FIH on 2-OG availability and the ability of DMOG to inhibit both PHD2 and FIH, suggest that DMOG's potent effect here may be via inhibition of both hydroxylases, whereas $CoCl_2$ and DFX may inhibit PHD2 only.

The ability of DMOG to induce an expression profile that is conducive for articular chondrogenesis, suggests its advantage over $CoCl_2$ and DFX for use in cartilage-regenerative therapies. However, despite inducing expression of *COL2A1* and genes involved in post-translational modifications of collagen, DMOG had a negative effect on cartilage-like ECM production. We showed that this was partly mediated via HIF-1α, however, other mechanisms are likely involved as we were unable to completely rescue cartilage-like ECM formation with Acriflavine. DMOG has been shown to reduce the activity of prolyl-4-hydroxylase, which is required for correct folding and polymerisation of collagen fibrils [21]. Correspondingly, both FIH and Collagen Prolyl Hydroxylase (P4HA1) have similar affinities for 2-OG, as they have similar K_m values for this co-factor [47]. Therefore, FIH and P4HA1 are likely equally sensitive to DMOG. This suggests that DMOG-mediated upregulation of HIF target genes via FIH inhibition might be accompanied by a similarly potent inhibition of collagen processing and incorporation into the ECM. Treatment with DMOG for the final 7 days of induction restored the reduced levels of Collagen Type II whilst upregulating expression of HIF target and chondrogenic genes to similar levels we observed in response to

continuous treatment. This response could have been mediated by a lack of continuous inhibition of the collagen prolyl hydroxylase. Taken together, late DMOG treatment, which can stimulate the formation of appropriate ECM, and induce mRNA expression of genes similarly to continuous treatment, may be a valuable strategy for cartilage regenerative medicine.

Conclusion

Hydroxylase inhibitors are potentially valuable in cartilage tissue engineering strategies as they can mimic many of the effects of hypoxia, providing important environmental cues to progenitors, but without many of its potential drawbacks. Here, we show that $CoCl_2$, DFX and DMOG treatment all induced HIF-1α stabilisation. However, unlike $CoCl_2$ and DFX, DMOG treatment strongly regulated HIF targets, and promoted chondrocyte-specific gene expression. This suggests that in hBM-MSC undergoing chondrogenic differentiation, HIF-mediated changes in gene expression may rely more on mechanisms that utilise 2-OG than those that rely on Fe^{2+}. Our observations also suggest a role for DMOG in cartilage tissue engineering strategies. For example, scaffolds that spatially and/or temporally control the release of DMOG could target the articular cartilage to aid in the repair of focal defects. However, the maintenance of cartilage ECM in late treatment-only conditions suggests the use of this 2-OG analogue would need to be optimised with regards to dosage/treatment time. Alternatively, knowledge that DMOG inhibits both FIH and PHD2 may suggest that dual and specific inhibition of these hydroxylases during *de novo* cartilage formation, may result in HIF-mediated transcription that is conducive for articular chondrogenesis.

Acknowledgements

DKT acknowledges a PhD studentship from Orthopaedic Research UK and was part funded by the Rosetrees Trust. HWA was supported by Cancer Research UK Clinician Scientist Fellowship (C41494/A15448). Support from the National Institute of Health Research Imperial Biomedical Research Centre, and the Imperial College London Healthcare Tissue Bank are also acknowledged. EG acknowledges a Research Career Development Fellowship from the Wellcome Trust and a Philip Leverhulme Prize from the Leverhulme Trust.
The authors wish to thank Ms. Angela Gates for administrative assistance and Dr. Chris Healy and Ms. Susmitha Rao for technical support.

Disclosure of potential conflicts of interests

The authors declare no conflict of interests.

References

1. Kreuz PC, Steinwachs MR, Erggelet C, Krause SJ, Konrad G, Uhl M, Sudkamp N: Results after microfracture of full-thickness chondral defects in different compartments in the knee. *Osteoarthritis Cartilage* 2006, 14**:**1119-1125.
2. Peterson L, Minas T, Brittberg M, Nilsson A, Sjogren-Jansson E, Lindahl A: Two- to 9-year outcome after autologous chondrocyte transplantation of the knee. *Clin Orthop Relat Res* 2000**:**212-234.
3. Wong KL, Lee KB, Tai BC, Law P, Lee EH, Hui JH: Injectable cultured bone marrow-derived mesenchymal stem cells in varus knees with cartilage defects undergoing high tibial osteotomy: a prospective, randomized controlled clinical trial with 2 years' follow-up. *Arthroscopy* 2013, 29**:**2020-2028.
4. Tamaddon M, Burrows M, Ferreira SA, Dazzi F, Apperley JF, Bradshaw A, Brand DD, Czernuszka J, Gentleman E: Monomeric, porous type II collagen scaffolds promote chondrogenic differentiation of human bone marrow mesenchymal stem cells in vitro. *Scientific Reports* 2017, 7.
5. McCullen SD, Autefage H, Callanan A, Gentleman E, Stevens MM: Anisotropic Fibrous Scaffolds for Articular Cartilage Regeneration. *Tissue Engineering Part A* 2012, 18**:**2073-2083.
6. Schipani E, Ryan HE, Didrickson S, Kobayashi T, Knight M, Johnson RS: Hypoxia in cartilage: HIF-1alpha is essential for chondrocyte growth arrest and survival. *Genes Dev* 2001, 15**:**2865-2876.
7. Provot S, Zinyk D, Gunes Y, Kathri R, Le Q, Kronenberg HM, Johnson RS, Longaker MT, Giaccia AJ, Schipani E: Hif-1alpha regulates differentiation of limb bud mesenchyme and joint development. *J Cell Biol* 2007, 177**:**451-464.
8. Hewitson KS, Lienard BM, McDonough MA, Clifton IJ, Butler D, Soares AS, Oldham NJ, McNeill LA, Schofield CJ: Structural and mechanistic studies on the inhibition of the hypoxia-inducible transcription factor hydroxylases by tricarboxylic acid cycle intermediates. *J Biol Chem* 2007, 282**:**3293-3301.
9. Wang GL, Semenza GL: General involvement of hypoxia-inducible factor 1 in transcriptional response to hypoxia. *Proc Natl Acad Sci U S A* 1993, 90**:**4304-4308.
10. Behrens J, von Kries JP, Kuhl M, Bruhn L, Wedlich D, Grosschedl R, Birchmeier W: Functional interaction of beta-catenin with the transcription factor LEF-1. *Nature* 1996, 382**:**638-642.
11. Robins JC, Akeno N, Mukherjee A, Dalal RR, Aronow BJ, Koopman P, Clemens TL: Hypoxia induces chondrocyte-specific gene expression in mesenchymal cells in association with transcriptional activation of Sox9. *Bone* 2005, 37**:**313-322.
12. Duval E, Bauge C, Andriamanalijaona R, Benateau H, Leclercq S, Dutoit S, Poulain L, Galera P, Boumediene K: Molecular mechanism of hypoxia-induced chondrogenesis and its application in in vivo cartilage tissue engineering. *Biomaterials* 2012, 33**:**6042-6051.
13. Amarilio R, Viukov SV, Sharir A, Eshkar-Oren I, Johnson RS, Zelzer E: HIF1alpha regulation of Sox9 is necessary to maintain differentiation of hypoxic prechondrogenic cells during early skeletogenesis. *Development* 2007, 134**:**3917-3928.
14. Aro E, Khatri R, Gerard-O'Riley R, Mangiavini L, Myllyharju J, Schipani E: Hypoxia-inducible factor-1 (HIF-1) but not HIF-2 is essential for hypoxic induction of collagen prolyl 4-hydroxylases in primary newborn mouse epiphyseal growth plate chondrocytes. *J Biol Chem* 2012, 287**:**37134-37144.

15. Makris EA, Responte DJ, Paschos NK: Developing functional musculoskeletal tissues through hypoxia and lysyl oxidase-induced collagen cross-linking. 2014, 111**:**E4832-4841.
16. Thoms BL, Dudek KA, Lafont JE, Murphy CL: Hypoxia promotes the production and inhibits the destruction of human articular cartilage. *Arthritis Rheum* 2013, 65**:**1302-1312.
17. Duval E, Leclercq S, Elissalde JM, Demoor M, Galera P, Boumediene K: Hypoxia-inducible factor 1alpha inhibits the fibroblast-like markers type I and type III collagen during hypoxia-induced chondrocyte redifferentiation: hypoxia not only induces type II collagen and aggrecan, but it also inhibits type I and type III collagen in the hypoxia-inducible factor 1alpha-dependent redifferentiation of chondrocytes. *Arthritis Rheum* 2009, 60**:**3038-3048.
18. Appelhoff RJ, Tian YM, Raval RR, Turley H, Harris AL, Pugh CW, Ratcliffe PJ, Gleadle JM: Differential function of the prolyl hydroxylases PHD1, PHD2, and PHD3 in the regulation of hypoxia-inducible factor. *J Biol Chem* 2004, 279**:**38458-38465.
19. Lando D, Peet DJ, Gorman JJ, Whelan DA, Whitelaw ML, Bruick RK: FIH-1 is an asparaginyl hydroxylase enzyme that regulates the transcriptional activity of hypoxia-inducible factor. *Genes Dev* 2002, 16**:**1466-1471.
20. Huang Z, He G, Huang Y: Deferoxamine synergizes with transforming growth factor-beta signaling in chondrogenesis. *Genet Mol Biol* 2017, 40**:**698-702.
21. Thoms BL, Murphy CL: Inhibition of hypoxia-inducible factor-targeting prolyl hydroxylase domain-containing protein 2 (PHD2) enhances matrix synthesis by human chondrocytes. *J Biol Chem* 2010, 285**:**20472-20480.
22. Nguyen LK, Cavadas MA, Scholz CC, Fitzpatrick SF, Bruning U, Cummins EP, Tambuwala MM, Manresa MC, Kholodenko BN, Taylor CT, Cheong A: A dynamic model of the hypoxia-inducible factor 1alpha (HIF-1alpha) network. *J Cell Sci* 2013, 126**:**1454-1463.
23. Wang GL, Semenza GL: Desferrioxamine induces erythropoietin gene expression and hypoxia-inducible factor 1 DNA-binding activity: implications for models of hypoxia signal transduction. *Blood* 1993, 82**:**3610-3615.
24. Tian YM, Yeoh KK, Lee MK, Eriksson T, Kessler BM, Kramer HB, Edelmann MJ, Willam C, Pugh CW, Schofield CJ, Ratcliffe PJ: Differential sensitivity of hypoxia inducible factor hydroxylation sites to hypoxia and hydroxylase inhibitors. *J Biol Chem* 2011, 286**:**13041-13051.
25. Bouaziz W, Sigaux J, Modrowski D, Devignes CS, Funck-Brentano T, Richette P, Ea HK, Provot S, Cohen-Solal M, Hay E: Interaction of HIF1alpha and beta-catenin inhibits matrix metalloproteinase 13 expression and prevents cartilage damage in mice. *Proc Natl Acad Sci U S A* 2016, 113**:**5453-5458.
26. Lv F-J, Tuan RS, Cheung KMC, Leung VYL: Concise Review: The Surface Markers and Identity of Human Mesenchymal Stem Cells. *STEM CELLS* 2014, 32**:**1408-1419.
27. Lin C, McGough R, Aswad B, Block JA, Terek R: Hypoxia induces HIF-1alpha and VEGF expression in chondrosarcoma cells and chondrocytes. *J Orthop Res* 2004, 22**:**1175-1181.
28. Metzen E, Stiehl DP, Doege K, Marxsen JH, Hellwig-Burgel T, Jelkmann W: Regulation of the prolyl hydroxylase domain protein 2 (phd2/egln-1) gene: identification of a functional hypoxia-responsive element. *Biochem J* 2005, 387**:**711-717.
29. Semenza GL, Roth PH, Fang HM, Wang GL: Transcriptional regulation of genes encoding glycolytic enzymes by hypoxia-inducible factor 1. *J Biol Chem* 1994, 269**:**23757-23763.

30. Akiyama H, Chaboissier MC, Martin JF, Schedl A, de Crombrugghe B: The transcription factor Sox9 has essential roles in successive steps of the chondrocyte differentiation pathway and is required for expression of Sox5 and Sox6. *Genes Dev* 2002, 16**:**2813-2828.
31. Zheng Q, Zhou G, Morello R, Chen Y, Garcia-Rojas X, Lee B: Type X collagen gene regulation by Runx2 contributes directly to its hypertrophic chondrocyte-specific expression in vivo. *J Cell Biol* 2003, 162**:**833-842.
32. Woo KJ, Lee TJ, Park JW, Kwon TK: Desferrioxamine, an iron chelator, enhances HIF-1alpha accumulation via cyclooxygenase-2 signaling pathway. *Biochem Biophys Res Commun* 2006, 343**:**8-14.
33. Befani C, Mylonis I, Gkotinakou IM, Georgoulias P, Hu CJ, Simos G, Liakos P: Cobalt stimulates HIF-1-dependent but inhibits HIF-2-dependent gene expression in liver cancer cells. *Int J Biochem Cell Biol* 2013, 45.
34. Groenman FA, Rutter M, Wang J, Caniggia I, Tibboel D, Post M: Effect of chemical stabilizers of hypoxia-inducible factors on early lung development. *Am J Physiol Lung Cell Mol Physiol* 2007, 293**:**L557-567.
35. Komori T, Yagi H, Nomura S, Yamaguchi A, Sasaki K, Deguchi K, Shimizu Y, Bronson RT, Gao YH, Inada M, et al: Targeted disruption of Cbfa1 results in a complete lack of bone formation owing to maturational arrest of osteoblasts. *Cell* 1997, 89**:**755-764.
36. Gleghorn L, Ramesar R, Beighton P, Wallis G: A mutation in the variable repeat region of the aggrecan gene (AGC1) causes a form of spondyloepiphyseal dysplasia associated with severe, premature osteoarthritis. *Am J Hum Genet* 2005, 77**:**484-490.
37. Reboul P, Pelletier JP, Tardif G, Cloutier JM, Martel-Pelletier J: The new collagenase, collagenase-3, is expressed and synthesized by human chondrocytes but not by synoviocytes. A role in osteoarthritis. *J Clin Invest* 1996, 97**:**2011-2019.
38. Lee K, Zhang H, Qian DZ, Rey S, Liu JO, Semenza GL: Acriflavine inhibits HIF-1 dimerization, tumor growth, and vascularization. *Proc Natl Acad Sci U S A* 2009, 106**:**17910-17915.
39. Niebler S, Angele P, Kujat R, Bosserhoff AK: Hypoxia-Inducible Factor 1 Is an Inductor of Transcription Factor Activating Protein 2 Epsilon Expression during Chondrogenic Differentiation. *Biomed Res Int* 2015, 2015**:**380590.
40. Gelse K, Pfander D, Obier S, Knaup KX, Wiesener M, Hennig FF, Swoboda B: Role of hypoxia-inducible factor 1 alpha in the integrity of articular cartilage in murine knee joints. *Arthritis Res Ther* 2008, 10**:**R111.
41. Arsham AM, Howell JJ, Simon MC: A novel hypoxia-inducible factor-independent hypoxic response regulating mammalian target of rapamycin and its targets. *J Biol Chem* 2003, 278**:**29655-29660.
42. Palomaki S, Pietila M, Laitinen S, Pesala J, Sormunen R, Lehenkari P, Koivunen P: HIF-1alpha is upregulated in human mesenchymal stem cells. *Stem Cells* 2013, 31**:**1902-1909.
43. Park IH, Kim KH, Choi HK, Shim JS, Whang SY, Hahn SJ, Kwon OJ, Oh IH: Constitutive stabilization of hypoxia-inducible factor alpha selectively promotes the self-renewal of mesenchymal progenitors and maintains mesenchymal stromal cells in an undifferentiated state. *Exp Mol Med* 2013, 45**:**e44.
44. Makris EA, Gomoll AH, Malizos KN, Hu JC, Athanasiou KA: Repair and tissue engineering techniques for articular cartilage. *Nat Rev Rheumatol* 2015, 11**:**21-34.
45. Leijten J, Georgi N, Moreira Teixeira L, van Blitterswijk CA, Post JN, Karperien M: Metabolic programming of mesenchymal stromal cells by oxygen tension directs chondrogenic cell fate. *Proc Natl Acad Sci U S A* 2014, 111**:**13954-13959.

46. Tarhonskaya H, Hardy AP, Howe EA, Loik ND, Kramer HB, McCullagh JS, Schofield CJ, Flashman E: Kinetic Investigations of the Role of Factor Inhibiting Hypoxia-inducible Factor (FIH) as an Oxygen Sensor. *J Biol Chem* 2015, 290**:**19726-19742.
47. Koivunen P, Hirsila M, Gunzler V, Kivirikko KI, Myllyharju J: Catalytic properties of the asparaginyl hydroxylase (FIH) in the oxygen sensing pathway are distinct from those of its prolyl 4-hydroxylases. *J Biol Chem* 2004, 279**:**9899-9904.

Figure Titles & Legends

Figure 1. Schematics highlighting the role of hydroxylase inhibitors in regulation of HIF-1α-mediated transcription and the study experimental design.

(A) Under hypoxic conditions, HIF-1α forms an active transcription complex with HIF-1β and co-factors such as CBP/p300. This HIF complex then binds to the promoter regions of target genes at the HIF-response element sites, inducing transcription.

(B) At normoxia, two hydroxylases – PHD2 and FIH, utilise oxygen and other substrates to hydroxylate HIF-1α which promotes its degradation and inhibitis binding by CBP/p300. Here, we aimed to stabilise HIF-1α at normoxia by inhibiting the hydroxylases with $CoCl_2$, DFX or DMOG.

(C) Experiment design. To produce each biological replicate, hBM-MSCs were thawed and expanded to passage 5 before re-seeding at a density of $3x10^4$ cell/cm^2 in multi-well plates. Each well or set of wells was assigned to a specific condition: 20%O_2, 20%O_2+$CoCl_2$, 20%O_2+DFX, 20%O_2+DMOG or 5%O_2. Separate experiments included each HIF-stabilising compound in the presence or absence of Acriflavine (ACF), and a comparison of late with constitutive exposure. In each condition, cultures were chondrogenically differentiated before assays at the time points specified in the legend of each figure.

Figure 2. Hypoxia induces HIF-1α nuclear localisation and promotes an articular chondrocyte-like phenotype.

(A+B) mRNA expression of *VEGFA*, *EGLN* and *PGK1*, and *SOX9* (n=4) at day 1 (A) and *SOX9*, *COL2A1* and *COL10A1* (n=8) at day 14 of chondrogenesis (B). Values plotted are fold change in response to 5%O_2 compared to 20%O_2, which is represented by the horizontal dotted line. The solid grey line represents the mean. *denotes $p<0.05$ compared to 20%O_2.

(C) hBM-MSC number throughout chondrogenesis as determined by PicoGreen assay (n=3). Values are normalised to cell number at day 0 and error bars show standard error of the mean.
(D) Quantification of nuclear HIF-1α immunofluorescence in F-H at day 1 of chondrogenesis (n=3). Each value represents the percentage of a single nucleus that is occupied by HIF-1α. The red horizontal line represents the mean with *p<0.05 compared to 20%O_2.
(E-H) HIF-1α immunofluorescent staining. Scale Bar = 50μm. Representative images of 3 independent repeats. Images were cropped and magnified to visualise localisation of HIF-1α.
(I+J) Alcian Blue staining for GAGs with haematoxylin counterstain at day 21 of chondrogenesis (n=3). Scale bar = 400μm.
(K-N) Collagen Type II (K+L) and X (M+N) immunofluorescence staining at day 21 of chondrogenesis (n=3). Scale bar = 400μm. Brightness and contrast were adjusted to an equal degree between all conditions.

Figure 3. $CoCl_2$, DFX and DMOG increase nuclear localisation of HIF-1α but only DMOG induces stable upregulation of HIF targets.
(A+B) Detection of HIF-1α and housekeeping protein, β-Actin by Western Blot analysis of whole-cell lysates from hBM-MSCs at day 1 of chondrogenesis (**A**; n=4). Western blots were quantified and normalised to levels of β-Actin (**B;** n=4). Values are magnitude difference compared to the no treatment control, which is represented by the horizontal dotted line. Solid coloured lines are the mean for each condition.
(C) Quantification of nuclear HIF-1α immunofluorescence at day 1 of chondrogenesis (n=4). Each value represents the percentage of a single nucleus that is occupied by HIF-1α. The red horizontal line represents the mean and *p<0.05 compared to 20%O_2.
(D-K) HIF-1α immunofluorescence staining at day 1 of chondrogenesis (n=4). Scale Bar = 50μm. Images were cropped and magnified to visualise localisation of HIF-1α. Brightness

and contrast were adjusted to an equal degree between all conditions.

(L-N) mRNA expression of *VEGFA*, *PGK1* and *EGLN* due to $CoCl_2$, DFX, DMOG and $5\%O_2$ (n=4). Values are fold change compared to the no treatment control represented by the horizontal dotted line. Solid coloured lines represent the mean for each condition. *p<0.05 compared to $20\%O_2$ at the same time point.

Figure 4. DMOG induces a chondrogenic transcriptional profile and inhibits markers of osteoblastic and hypertrophic differentiation but also reduces the formation of a cartilage-like ECM.

(A-J) mRNA expression of *SOX9* (A; n=4), *RUNX2* (B; n=4) and *SOX9*/RUNX2 (C; n=4), *COL2A1* (D; n=7), *COL10A1* (E; n=7), *COL2A1*/*COL10A1* (F; n=7), *ACAN* (G; n=4), *MMP13* (H; n=7), *P4HA1* (I; n=4) and *LOX* (J; n=7) throughout chondrogenesis due to treatment with $CoCl_2$, DFX, DMOG and $5\%O_2$. Values are fold change compared to the no-treatment control represented by the horizontal dotted line. Solid coloured lines are the mean for each condition. *p<0.05 compared to $20\%O_2$ at the same time point.

Figure 5. DMOG reduces the formation of a cartilage-like ECM.

(A-H) Collagen Type X (A-D) and II (E-H) immunofluorescence staining at day 21 of chondrogenesis (n=3). Scale bar = 400µm. Brightness and contrast were adjusted to an equal degree between all conditions.

(I-L) Alcian Blue staining for GAGs with haematoxylin counterstain at day 21 of chondrogenesis (n=3). Scale bar = 400µm.

(M+N) Quantification of Collagen Type II immunofluorescence (M) and Glycosaminoglycans (N) at day 21 of chondrogenesis (n=4) without (○/○/○) and with (●/●/●) normalisation to DAPI-immunofluorescence/double-stranded DNA. Values are fold change

compared to the no-treatment control represented by the horizontal dotted line. Solid coloured lines represent means for each condition. *p<0.05 compared to 20%O_2.

Figure 6. Inhibition of HIF-1α reduces the DMOG-mediated upregulation of a chondrogenic transcriptional profile

(A-C) Collagen Type II immunofluorescence staining at day 14 of chondrogenesis. Scale bar = 400μm (n=4). Brightness and contrast were adjusted to an equal degree between all conditions.

(D) Quantification of Collagen Type II immunofluorescence at day 14 of chondrogenic induction, normalised to equivalent DAPI-immunofluorescence (n=4). Values are fold change compared to the no-treatment control represented by the horizontal dotted line. Orange lines represent means for each condition. *p<0.05 compared to 20%O_2.

(E-J) mRNA expression of *VEGFA* (E) and *EGLN* (F), *SOX9* (G), *COL2A1* (H), *COL10A1* (I), and *COL2A1*/*COL10A1* (J) at day 14 of chondrogenesis (n=4) after treatment with DMOG (●), 5%O_2 (●), DMOG + Acriflavine (○) or 5%O_2 + Acriflavine (○). Values are fold change compared to the no-treatment condition represented by the horizontal dotted line. Solid coloured lines represent means for each condition. *p<0.05 when compared to 20%O_2, and $^{\#}p$<0.05 between +/-ACF conditions within 20%O_2 + DMOG or 5%O_2 groups.

Figure 7. Late DMOG treatment does not inhibit the formation of a Collagen Type II-rich ECM but does induce a chondrogenic expression profile.

(A-G) Collagen Type II immunofluorescence staining at day 21 of chondrogenesis after continuous (days 1-21) and late (days 14-21) $CoCl_2$, DFX and DMOG treatment (n=4). Scale bar = 400μm. Representative images from 4 independent repeats shown. Brightness and contrast were adjusted for all channels to an equal degree between all conditions.

(H) Quantification of Collagen Type II immunofluorescence at day 21 of chondrogenic induction, normalised to equivalent DAPI-immunofluorescence (n=4). Values are fold change compared to the no-treatment control represented by the horizontal dotted line. The horizontal, coloured lines represent means for each condition. **p*<0.05 compared to 20%O_2. **(I-L)** mRNA expression of *SOX9* (I), *P4HA1* (J), *VEGFA* (K) and *EGLN* (L) after continuous (days 1-21) and late (days 14-21) $CoCl_2$, DFX and DMOG treatment (n=4). Values are normalised to the housekeeping gene *RPL13A* and are fold change compared to the no-treatment control, represented by the horizontal dotted line. The horizontal coloured lines represent the means for each condition. **p*<0.05 when compared to 20%O_2.

Supplemental Figure 1. Primary antibody validation in hBM-MSC.

(A, B, D, E, G, H) Immunofluorescence signal following immunostaining protocol in which the primary antibody was included.

(C, F, I) Immunofluorescence signal following immunostaining protocol in which the primary antibody was omitted.

(A-C) HIF-1α: 20%O_2 (A) + 5%O_2 (B+C) at day 1 of chondrogenesis. Scale bar = 100μm.

(D-F) Collagen Type II: 20%O_2 at days 0 (D) and 21 (E+F) of chondrogenesis. Scale bar = 200μm.

(G-I) Collagen Type X: 5%O_2 (G) and 20%O_2 (H+I) at day 21 of chondrogenesis. Scale bar = 200μm.

Supplemental Figure 2. Determination of appropriate concentrations of $CoCl_2$, DFX and DMOG that limit cell toxicity.

(A-C) Cell viability throughout 21-day chondrogenic differentiation with varying concentrations of $CoCl_2$ (**A**), DFX (**B**) and DMOG (**C**) included in the induction media. Values are normalised to cell number at day 0 and represent the mean of 3 independent repeats. Error bars show standard error of the mean.

Supplemental Figure 3. Cell number in control, 5%O_2-, $CoCl_2$-, DFX- and DMOG-treated cultures during chondrogenic differentiation of hBM-MSC.

Cell number during the chondrogenic differentiation of hBM-MSC in the presence of $CoCl_2$, DFX, DMOG or 5%O_2. Values are normalised to cell number at day 0 and represent the mean of 3 independent repeats, with each repeat the mean of 3 technical replicates. Error bars show standard error of the mean.

Supplemental Figure 4. Effect of HIF-1α inhibition on mRNA expression of HIF target and chondrogenic genes. HIF-1α inhibition reduces DMOG's effects more strongly than that induced by $CoCl_2$, DFX or 5%O_2.

(A) Acriflavine (ACF) functional assay: Relative mRNA expression of HIF targets *VEGF*, *EGLN*, *PGK1*, and *GLUT2* in control, DMOG-treated and DMOG+ACF treated cultures. ACF abolishes DMOG-mediated upregulation of HIF targets. Values plotted are magnitude difference compared to the 20%O_2 condition.

(B) Total cell number determined by DAPI fluorescence at day 14 of DMOG-mediated chondrogenic differentiation in presence of ACF. Values plotted are magnitude difference to that without ACF, which is represented by the dotted line.

(C-H) mRNA expression levels represented in a heatmap of *SOX9* (C), *COL2A1* (D), *LOX* (E), *MMP13* (F), *COL10A1* (G), *EGLN* (H), and *VEGFA* (G) at day 14 of chondrogenesis after treatment with $CoCl_2$, DFX, DMOG or 5%O_2 in the absence and presence of Acriflavine (ACF). Values plotted are magnitude difference compared to untreated control within respective -ACF and +ACF groups and represent the mean from 4 independent experiments.

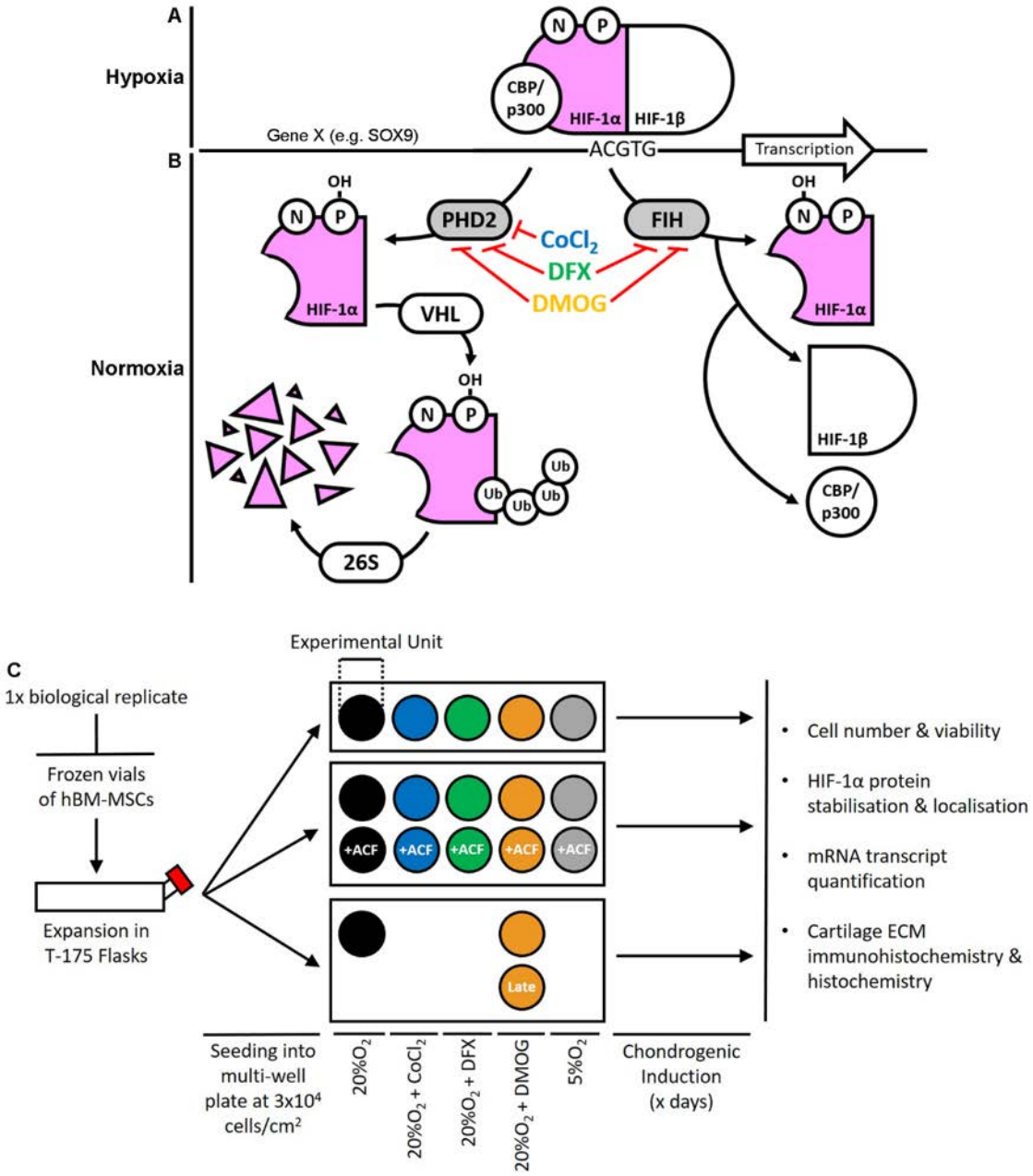
A
Hypoxia
N
P
CBP/
p300
HIF-1α
HIF-1β
Gene X (e.g. SOX9)
ACGTG
Transcription
B
Normoxia
OH
PHD2
CoCl2
DFX
DMOG
FIH
VHL
Ub
26S
C
1x biological replicate
Frozen vials
of hBM-MSCs
Expansion in
T-175 Flasks
Experimental Unit
+ACF
Late
Cell number & viability
HIF-1α protein
stabilisation & localisation
mRNA transcript
quantification
Cartilage ECM
immunohistochemistry &
histochemistry
Seeding into
multi-well
plate at 3x10^4
cells/cm^2
20%O2
20%O2 + CoCl2
20%O2 + DFX
20%O2 + DMOG
5%O2
Chondrogenic
Induction
(x days)

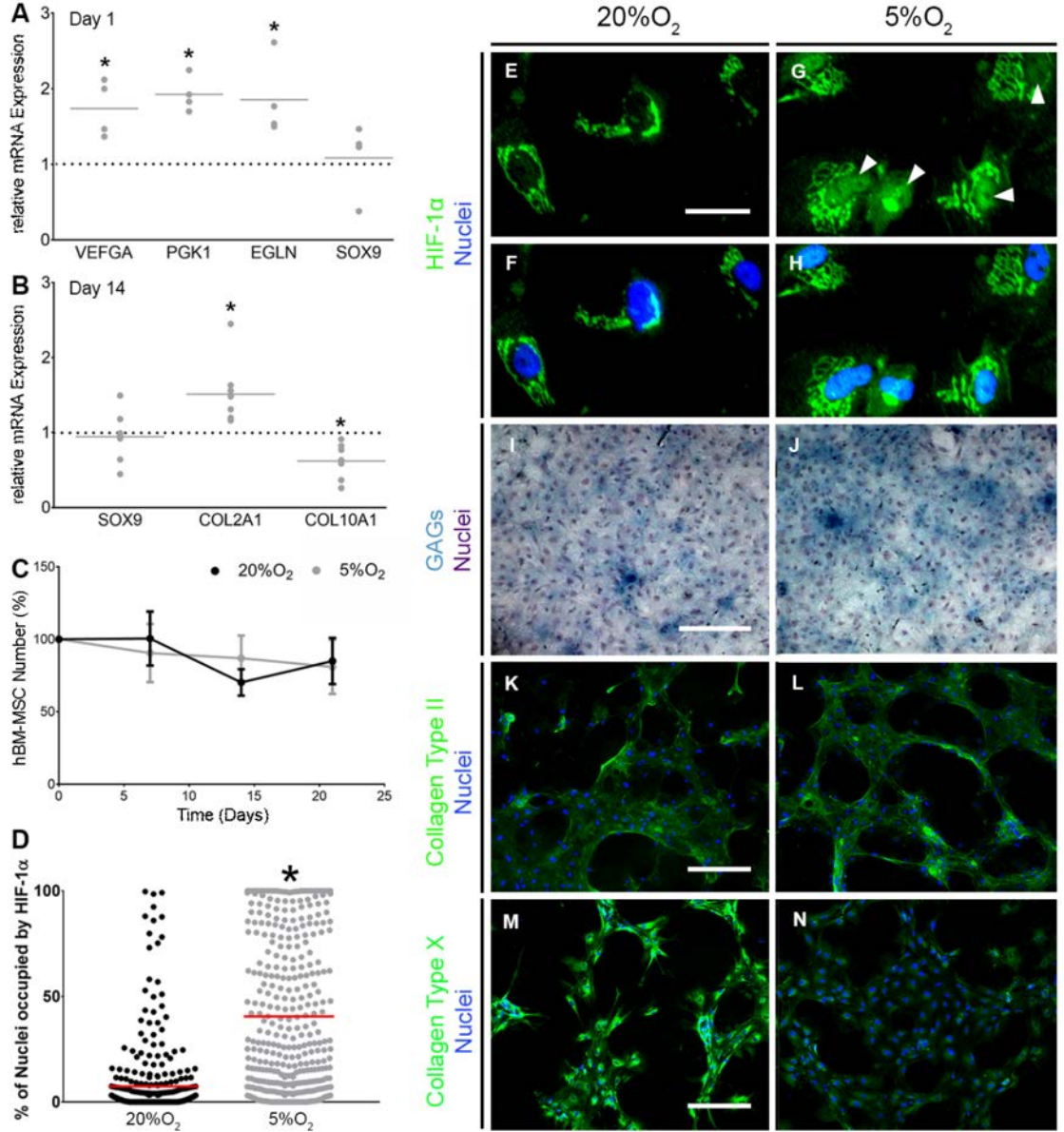
A
Day 1
relative mRNA Expression
VEFGA
PGK1
EGLN
SOX9
B
Day 14
relative mRNA Expression
SOX9
COL2A1
COL10A1
C
20%O2
5%O2
hBM-MSC Number (%)
Time (Days)
D
% of Nuclei occupied by HIF-1α
20%O2
5%O2
20%O2
5%O2
HIF-1α
Nuclei
GAGs
Nuclei
Collagen Type II
Nuclei
Collagen Type X
Nuclei
E
F
G
H
I
J
K
L
M
N

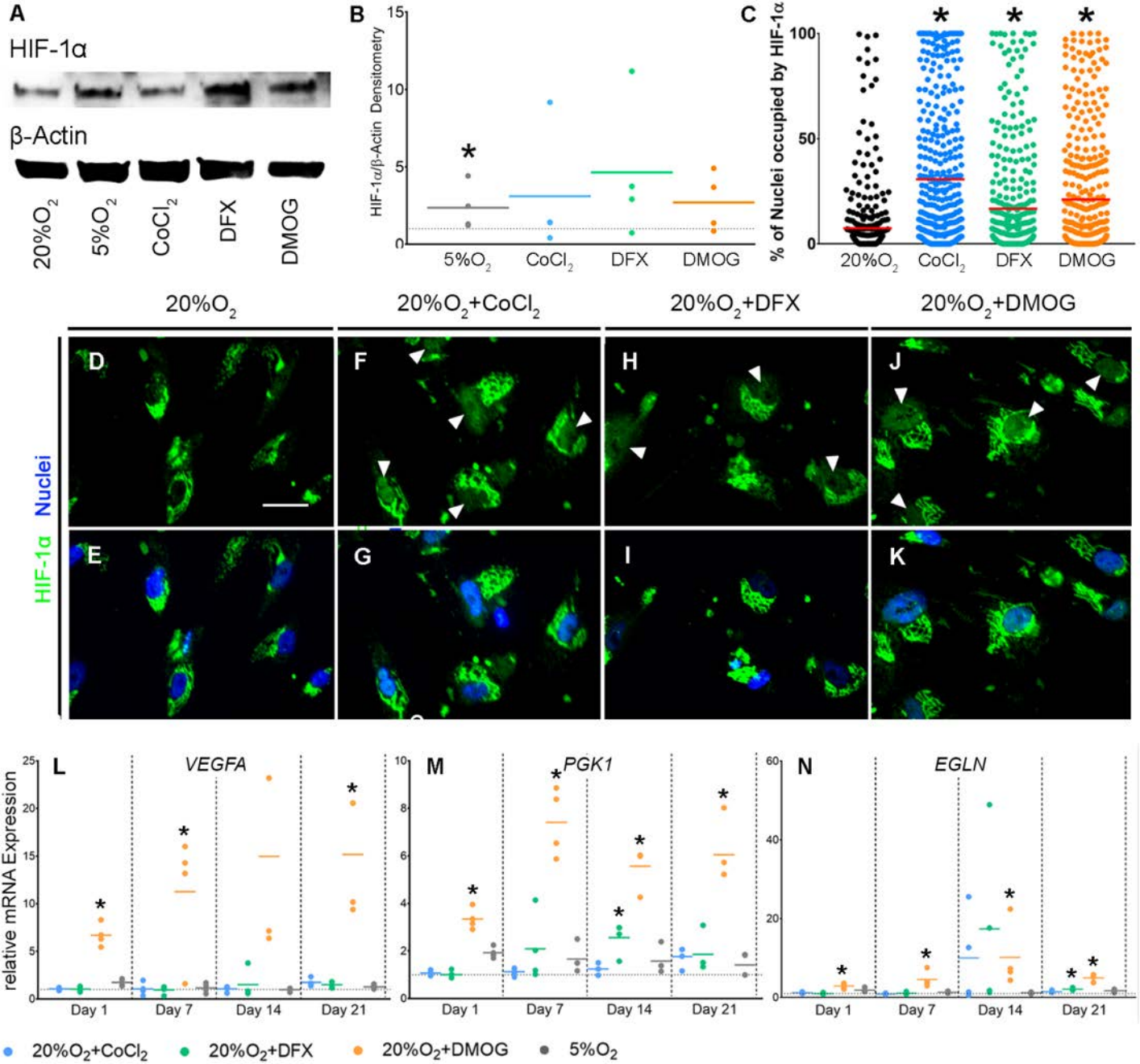
A
HIF-1α
β-Actin
20%O2
5%O2
CoCl2
DFX
DMOG
B
HIF-1α/β-Actin Densitometry
5%O2
CoCl2
DFX
DMOG
C
% of Nuclei occupied by HIF-1α
20%O2
CoCl2
DFX
DMOG
20%O2
20%O2+CoCl2
20%O2+DFX
20%O2+DMOG
Nuclei
HIF-1α
D
E
F
G
H
I
J
K
L
VEGFA
M
PGK1
N
EGLN
relative mRNA Expression
Day 1
Day 7
Day 14
Day 21
20%O2+CoCl2
20%O2+DFX
20%O2+DMOG
5%O2

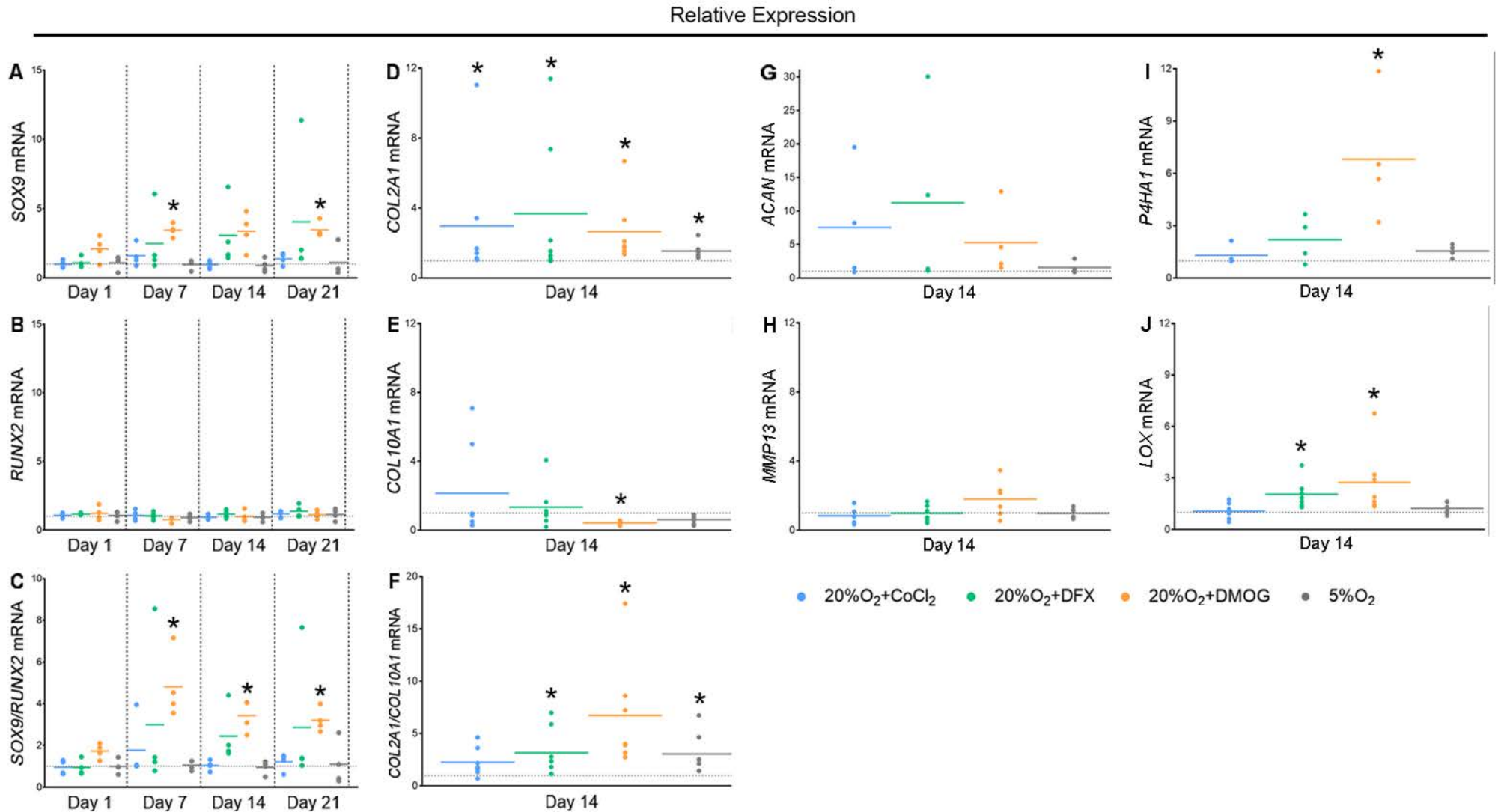
Relative Expression
A
SOX9 mRNA
Day 1
Day 7
Day 14
Day 21
B
RUNX2 mRNA
C
SOX9/RUNX2 mRNA
D
COL2A1 mRNA
Day 14
E
COL10A1 mRNA
F
COL2A1/COL10A1 mRNA
G
ACAN mRNA
H
MMP13 mRNA
I
P4HA1 mRNA
J
LOX mRNA
20%O2+CoCl2
20%O2+DFX
20%O2+DMOG
5%O2

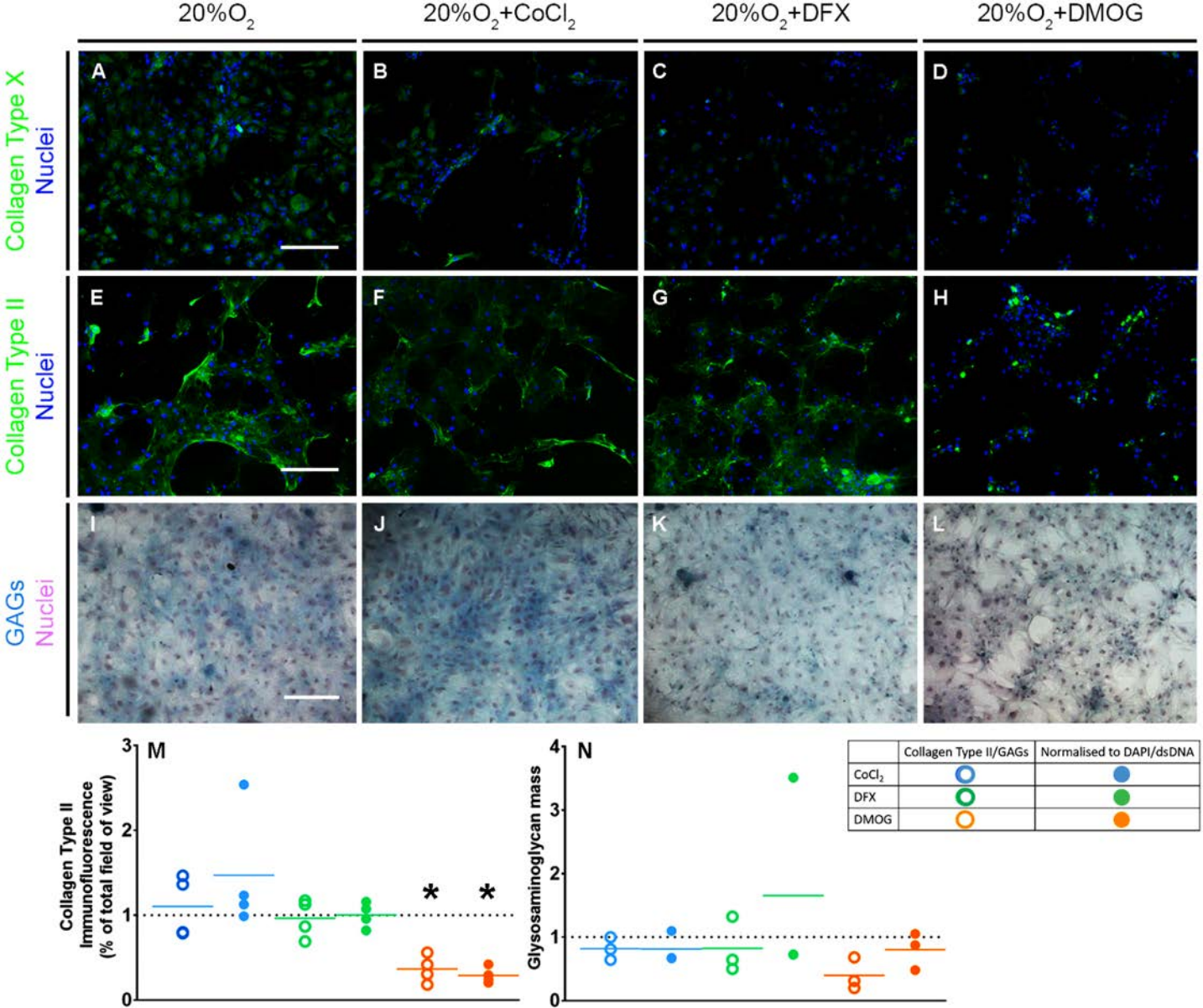
20%O2
20%O2+CoCl2
20%O2+DFX
20%O2+DMOG
Collagen Type X
Nuclei
Collagen Type II
Nuclei
GAGs
Nuclei
A
B
C
D
E
F
G
H
I
J
K
L
M
Collagen Type II Immunofluorescence (% of total field of view)
N
Glysosaminoglycan mass
Collagen Type II/GAGs
Normalised to DAPI/dsDNA
CoCl2
DFX
DMOG
*
*

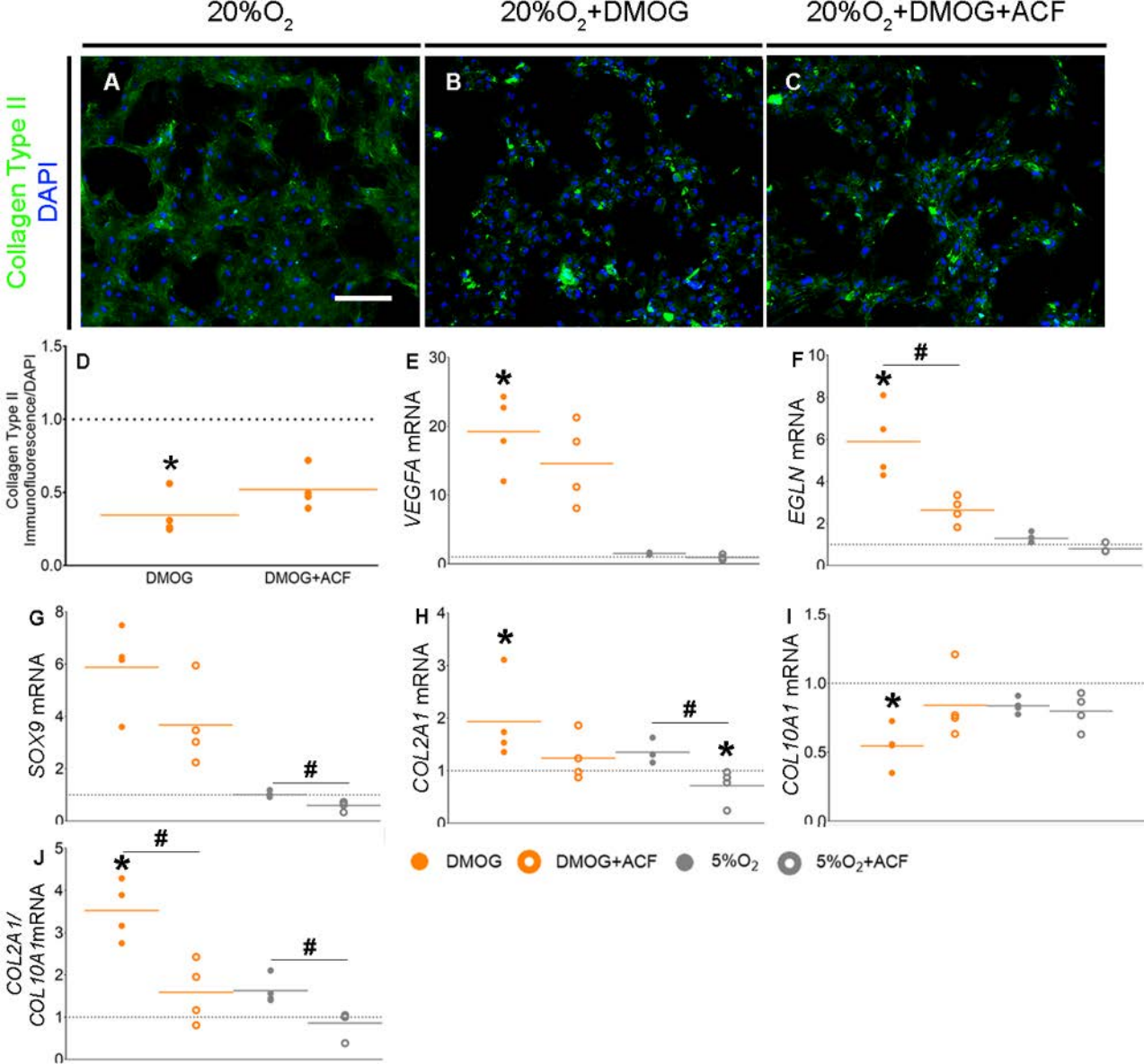
20%O2
20%O2+DMOG
20%O2+DMOG+ACF
Collagen Type II
DAPI
A
B
C
D
Collagen Type II Immunofluorescence/DAPI
DMOG
DMOG+ACF
E
VEGFA mRNA
F
EGLN mRNA
G
SOX9 mRNA
H
COL2A1 mRNA
I
COL10A1 mRNA
J
COL2A1/ COL10A1mRNA
DMOG
DMOG+ACF
5%O2
5%O2+ACF

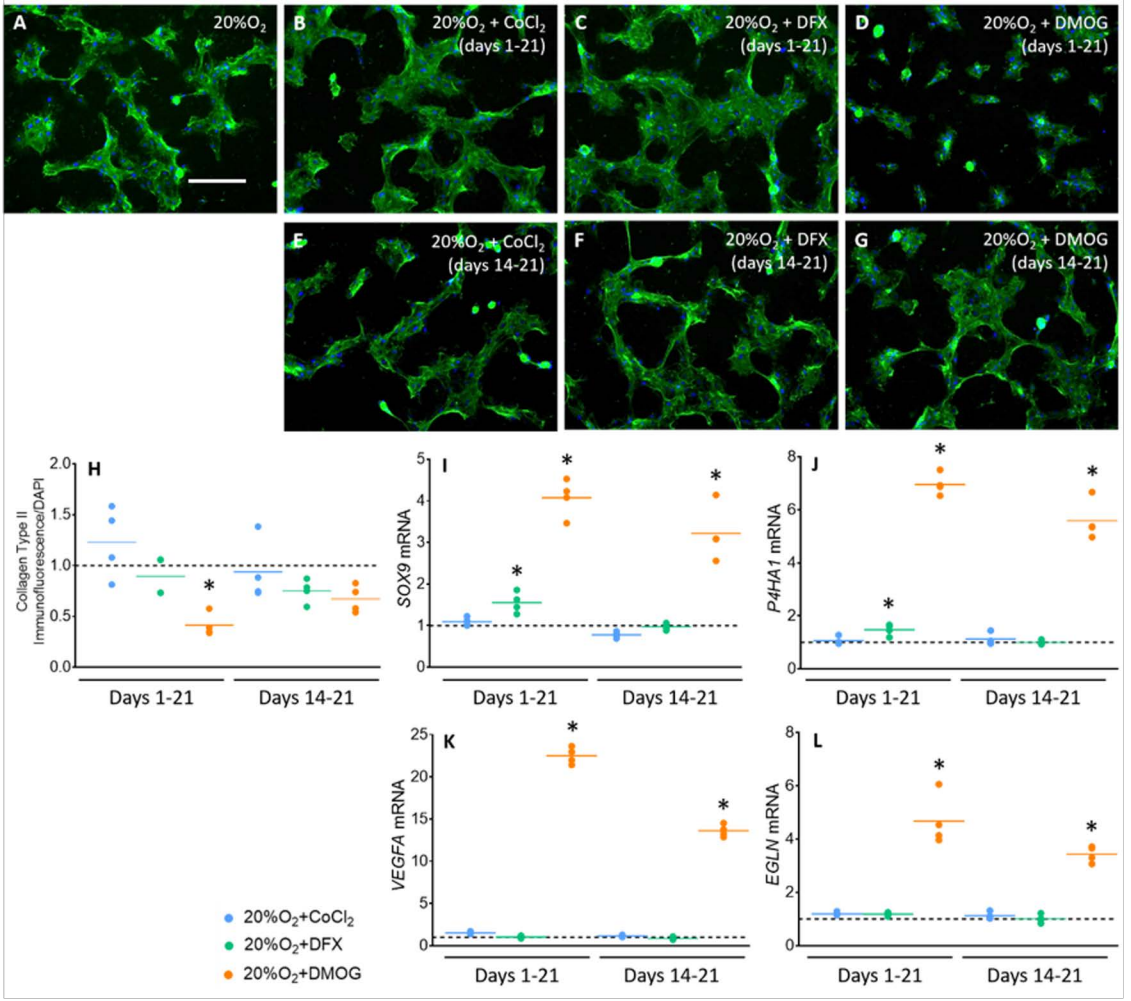
A
20%O2
B
20%O2 + CoCl2
(days 1-21)
C
20%O2 + DFX
(days 1-21)
D
20%O2 + DMOG
(days 1-21)
E
20%O2 + CoCl2
(days 14-21)
F
20%O2 + DFX
(days 14-21)
G
20%O2 + DMOG
(days 14-21)
H
Collagen Type II
Immunofluorescence/DAPI
Days 1-21
Days 14-21
I
SOX9 mRNA
Days 1-21
Days 14-21
J
P4HA1 mRNA
Days 1-21
Days 14-21
K
VEGFA mRNA
Days 1-21
Days 14-21
L
EGLN mRNA
Days 1-21
Days 14-21
20%O2+CoCl2
20%O2+DFX
20%O2+DMOG

A
B
C
HIF-1α
Nuclei
D
E
F
Collagen Type II
Nuclei
G
H
I
Collagen Type X
Nuclei

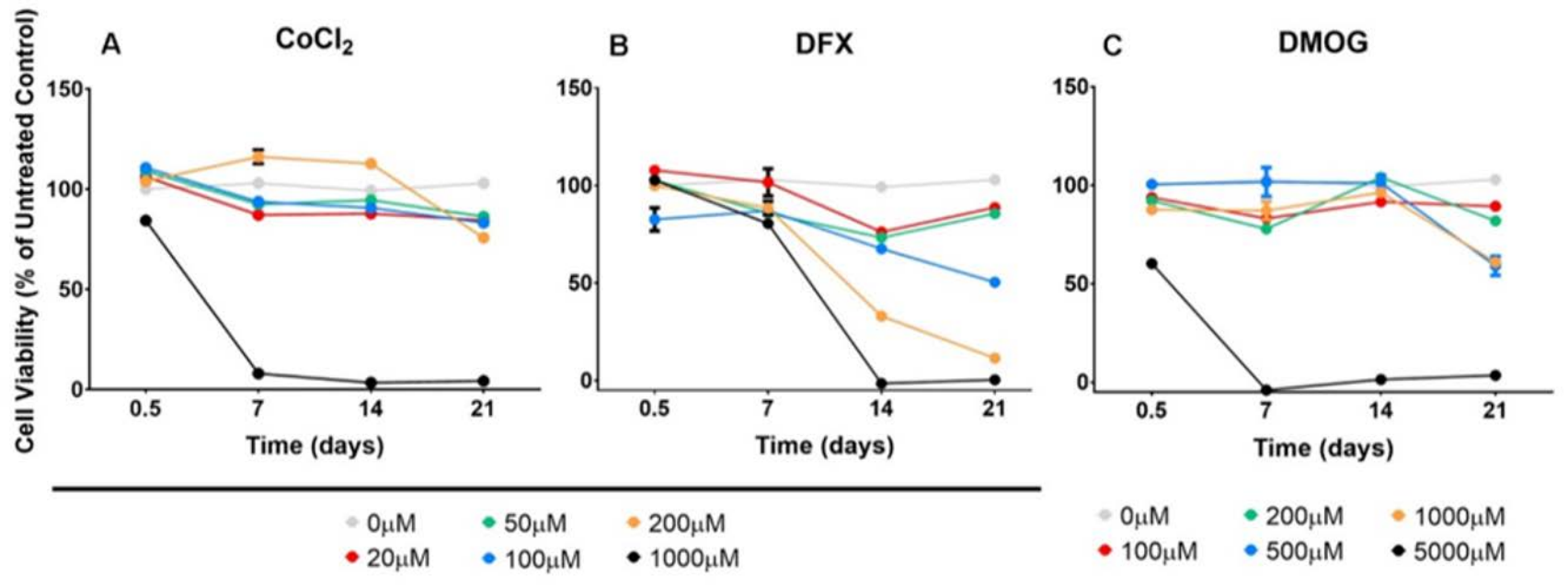
A
CoCl2
B
DFX
C
DMOG
Cell Viability (% of Untreated Control)
150
100
50
0
0.5
7
14
21
Time (days)
0μM
20μM
50μM
100μM
200μM
1000μM
0μM
100μM
200μM
500μM
1000μM
5000μM

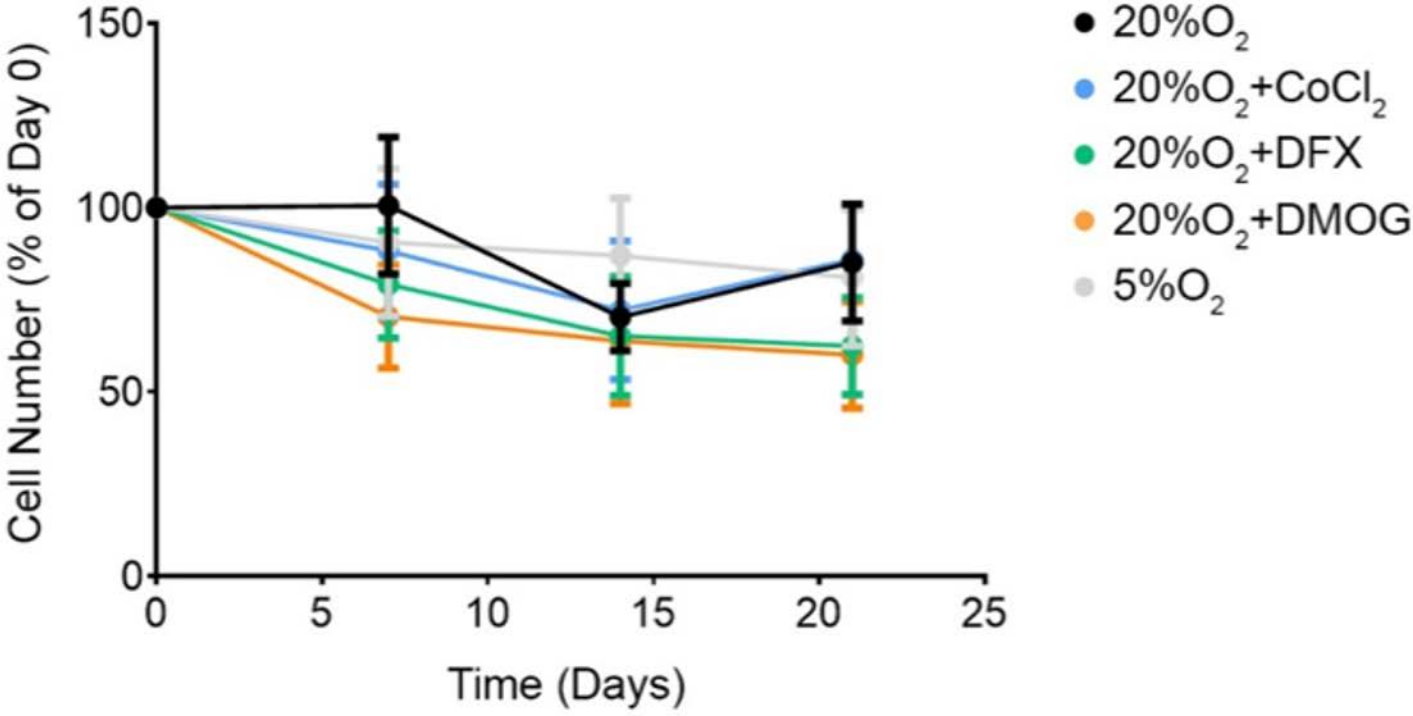
150
100
50
0
Cell Number (% of Day 0)
0
5
10
15
20
25
Time (Days)
20%O2
20%O2+CoCl2
20%O2+DFX
20%O2+DMOG
5%O2

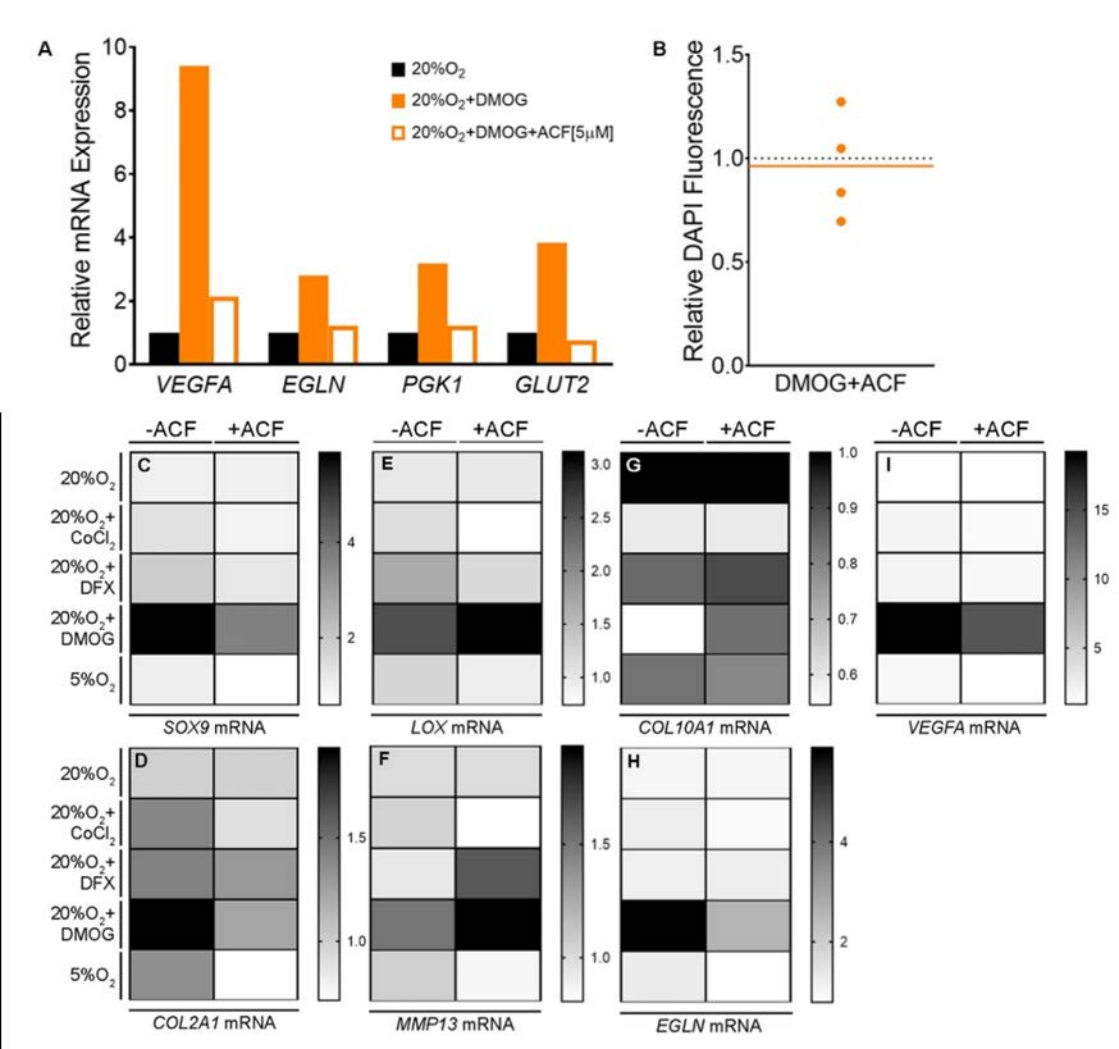
A
Relative mRNA Expression
20%O2
20%O2+DMOG
20%O2+DMOG+ACF[5μM]
VEGFA
EGLN
PGK1
GLUT2
B
Relative DAPI Fluorescence
DMOG+ACF
-ACF
+ACF
20%O2
20%O2+ CoCl2
20%O2+ DFX
20%O2+ DMOG
5%O2
C
SOX9 mRNA
D
COL2A1 mRNA
E
LOX mRNA
F
MMP13 mRNA
G
COL10A1 mRNA
H
EGLN mRNA
I
VEGFA mRNA

Supplemental Table 1. qPCR Primer Sequences

Gene of Interest	Forward Primer Sequence	Reverse Primer Sequence
VEGFA	AGGGCAGAATCATCACGAAGT	AGGGTCTCGATTGGATGGCA
PGK1	TGGACGTTAAAGGGAAGCGG	GCTCATAAGGACTACCGACTTGG
EGLN	AGGCGATAAGATCACCTGGAT	TTCGTCCGGCCATTGATTTTG
SOX9	AGCGAACGCACATCAAGAC	CTGTAGGCGATCTGTTGGGG
COL2A1	CCAGATGACCTTCCTACGCC	TTCAGGGCAGTGTACGTGAAC
ACAN	GTGCCTATCAGGACAAGGTCT	GATGCCTTTCACCACGACTTC
RUNX2	TGGTTACTGTCATGGCGGGTA	TCTCAGATCGTTGAACCTTGCTA
COL10A1	GGGGCTAAGGGTGAAAGGG	GGTCCTCCAACTCCAGGATCA
MMP13	ACTGAGAGGCTCCGAGAAATG	GAACCCCGCATCTTGGCTT
P4HA1	AGTACAGCGACAAAAGATCCAG	CTCCAACTCACTCCACTCAGTA
LOX	CGGCGGAGGAAAACTGTCT	TCGGCTGGGTAAGAAATCTGA
RPL13A	GCCATCGTGGCTAAACAGGTA	GTTGGTGTTCATCCGCTTGC